TRANSISTOR NOISE IN THE VERY HIGH FREQUENCY (VHF) RANGE

A Thesis

Presented to

The Faculty of Graduate Studies and Research

The University of Manitoba

In Partial Fulfillment

of the Requirements for the Degree

Master of Science in Electrical Engineering

by

Bisara Halil

October 1966

ABSTRACT

The purpose of this thesis is to investigate the validity of present noise theory of drift transistors at the frequency of 100 MHz., using the hybrid-Π model in a common emitter configuration.

The thesis contains the derivation of the noise figure for the hybrid-Π model, taking into account the cross-correlation between the noise generators. The derivation is based on VAN DER ZIEL's definition of the noise generators for the T model representation. (Ref.# 3).

ACKNOWLEDGEMENTS

The author wishes to express his gratitude to his thesis advisor, Professor A. Jakobschuk, for his guidance throughout the project; to the University of Manitoba for its financial assistance; and also to Mr. A. Kracikas for his technical assistance.

To my brother, Ilyas

TABLE OF CONTENTS

LIST OF FIGURES

LIST OF FIGURES (Continued...)

CHAPTER I

INTRODUCTION

Electrical noise is due to the discrete nature of electron flow and to the randomness of particle motion. This electrical noise can be divided into two groups: (1) noise caused by man (which can be controlled); and, (2) noise due to spontaneous fluctuations (which is beyond control). Spontaneous fluctuations of stationary nature can be described by two basic theorems, namely Nyquist's and Schottky's theorems.

Nyquist's Theorem:[6] In a conductor, the random vibration of ions about a normal or average position is a function of temperature. There is a continuous energy transfer due to collisions between the vibrating ions and the free electrons. Even though the average current is zero, random fluctations still exist. At temperature T, the thermal noise of a purely resistive circuit can be represented by noise generators. In a frequency range Δf, the generators deliver a maximum power (P) (called the available power) of

$$P = kT\Delta f \qquad \ldots (1)$$

where k is Boltzmann's constant, T is the temperature of the impedance in degrees Kelvin, and P is the power in watts. It was shown by Nyquist that the mean-square thermal noise voltage $\overline{e_s^2}$ generated by an impedance Z is given by:

$$\overline{e_s^2} = 4kTR\Delta f \qquad \ldots (2)$$

where R is the resistive part of the impedance Z in ohms. This noise generator may be represented by a Norton or a Thevenin-equivalent circuit:

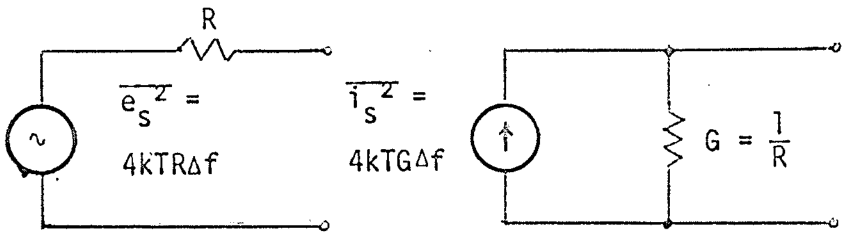

Figure 1

REPRESENTATION OF RESISTOR THERMAL NOISE

Schottky's Theorem:[6] This theorem deals with the random emission of current carriers in temperature-limited vacuum diodes. The individual current carriers are composed of a series of independent random events. Small variations in current may be represented by a noise-current generator in parallel with the noiseless incremental admittance of the diode. In a frequency interval Δf, the mean-square value of this generator is

$$\overline{i^2} = 2qI\Delta f \qquad \text{... (3)}$$

where I is the average plate current in amperes, and q is the electronic charge (1.6×10^{-19} coulombs).

In a transistor, shot noise is experienced in both junctions. Since the majority of the charge carriers pass through both the emitter-base junction and the collector-base junction, the two noise sources are correlated.

NOISE SOURCES IN TRANSISTORS

According to VAN DER ZIEL[5], all charge carriers which contribute noise to a npn transistor may be subdivided into eight groups:

(1) Electrons injected by the emitter and collected by the collector.

(2) Electrons injected by the emitter and recombining in the base region.

(3) Electrons injected into the base and returning to the emitter.

(4) Electrons trapped in the emitter space-charge region and recombining with holes coming from the base.

(5) Electrons trapped in the emitter space-charge region and returning to the emitter after being detrapped thermally.

(6) Electrons generated in the base and collected by the emitter.

(7) Electrons generated in the base and collected by the collector.

(8) Thermal fluctuation due to the extrinsic base resistance, $r_{bb'}$.

Each of the eight processes contribute noise in accordance with Schottky's or Nyquist's theorems. The noise contributions are:

From groups (1) and (2) the shot noise due to the emitter current I_E and due to the current I_{EE} :

$$2q\ (I_E + I_{EE})\Delta f$$

where I_{EE} is the current due to the electrons injected by the emitter and recombining in the base region.

From group (6) the shot noise due to the current I_{EE} :

$$2q\ I_{EE}\ \Delta f$$

and from groups (3) and (5) the thermal noise due to the real value of the emitter conductance g_e and due to the low frequency value of the emitter conductance g_{eo} :

$$4kT(g_e - g_{eo})\Delta f.$$

Thus the total noise current caused by the emitter current can be expressed as

$$\overline{i_1{}^2} = 4kT(g_e - g_{eo})\Delta f + 2q(I_E + 2I_{EE})\Delta f \qquad \dots (4)$$

Fluctuations in the d.c. current carried by the electrons of groups (1) and (7) can be represented by a noise current generator i_2 connected in parallel with the emitter-collector terminals with a mean square value of

$$\overline{i_2^2} = 2q\,\alpha_{dc}\,(I_E + I_{EE})\Delta f + 2qI_{CC}\Delta f \qquad \ldots (5)$$

where α_{dc} is the dc emitter efficiency and I_{CC} is the current due the electrons generated in the base and collected by the collector.

Since $\quad I_C = \alpha_{dc}\,(I_E + I_{EE}) + I_{CC}$

then

$$\overline{i_2^2} = 2qI_C\,\Delta f. \qquad \ldots (6)$$

DERIVATION OF THE HYBRID-Π NOISE MODEL

The electrical behaviour of the transistor, especially when it is used in a common-emitter configuration over a wide range of frequencies, can be represented by the widely used hybrid-Π model of Giacolletto-Johnson[16]. Thus, the noise performance of a common emitter npn transistor amplifier is best represented by a hybrid-Π model.

For small a.c. signals, the T-equivalent model of a common-emitter transistor configuration is as follows:

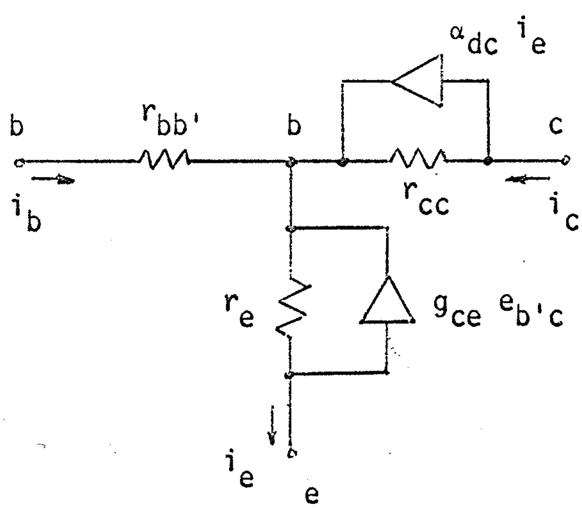

$$g_{ce} = \frac{1}{\lambda\ r_{cc}\ (1 - \alpha)}$$

Figure 2

REPRESENTATION OF A COMMON-EMITTER TRANSISTOR MODEL where b, b', c and e are the base, intrinsic base, collector and emitter terminals of a transistor, respectively; $r_{bb'}$ is the extrinsic base resistance, r_{cc} is the reverse junction resistance, g_{ce} is the feedback conductance which is a function of the emitter current I_E and the voltage V_{bc} , while λ is a constant which ranges from 2 to 5 for most transistors.[11]

The current generator αi_e in Figure 2 will yield several current generators when $i_e = -g_{ce}\, e_{b'c} + \frac{e_{b'e}}{r_e}$ is substituted. Now the current generator may be split into two parts. A few simplifications such as $g_m = \frac{\alpha}{r_e}$, $r_{b'e} = \frac{r_e}{1 - \alpha}$ and $e_{cb'} \cong e_{ce}$ will result in the following model

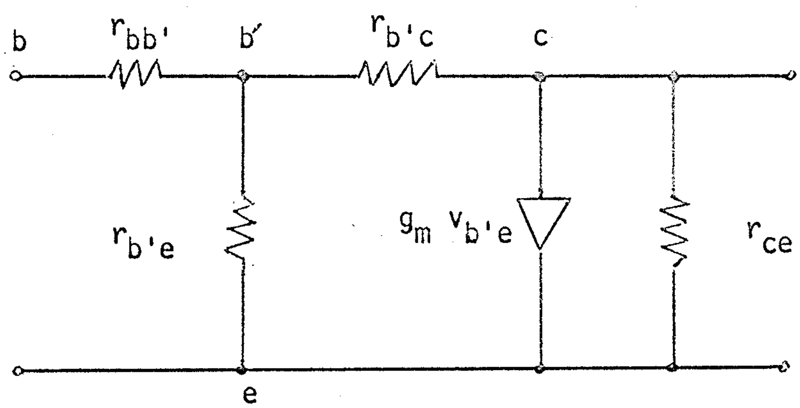

Figure 3

HYBRID-π MODEL OF A TRANSISTOR

where $$r_{ce} = \frac{1}{g_{ce}}$$ and

$$r_{b'c} = \frac{r_{cc}}{1 - g_{ce}\, r_{cc}(1 - \alpha)} .$$

The model of Figure 3 may be applicable over a wide range of frequencies. As the frequency increases, the effect of the capacitances should be considered. Therefore the model is modified to that of Figure 4.

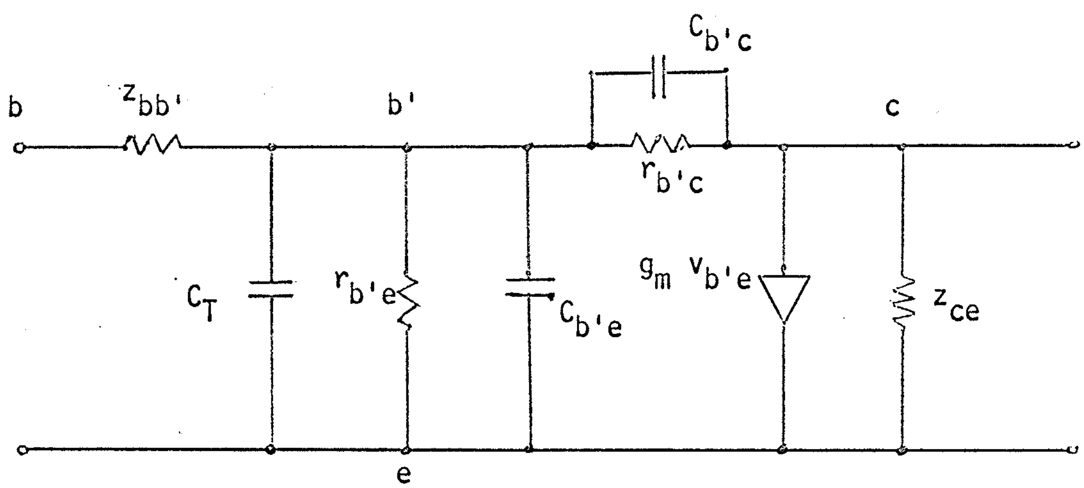

Figure 4

HIGH FREQUENCY HYBRID Π MODEL

At high frequencies, $r_{bb'}$ must be replaced by $z_{bb'}$ and as well $r_{b'e}$ by $z_{b'e}$ or z_{Π} ; $r_{b'c}$ by $z_{b'c}$ and r_{ce} by z_{ce} . The resistances $r_{b'c}$ and r_{ce} are large enough to be ignored at high frequencies. Ignoring r_{ce} implies a load impedance that is small compared to r_{ce}, whereas ignoring $r_{b'c}$ is a recognition of the fact that $r_{b'c}$ is large compared to the reactance of $C_{b'c}$. The capacitance $C_{b'e}$ is large enough at low frequencies to swamp the effects of the emitter-base transition capacitance C_T and, hence, C_T is ignored at low frequencies. But at high frequencies, the capacitance $C_{b'e}$ is not large enough to swamp the effect of C_T . Therefore, both capacitances $C_{b'e}$ and C_T should normally be kept separate.

Since the capacitance $C_{b'e}$ is directly proportional to the emitter current I_E , a low I_E will result in small values of $C_{b'e}$, which will enable the emitter-base transition capacitance C_T to be of major importance. But for large values of emitter current, C_T is normally ignored.

Various relationships that should be kept in mind are:

(a) $g_m r_{b'e} = \beta$ (β is the d.c. current gain and normally assumed independent of the Q point).

(b) $g_m = \frac{\alpha_{dc}}{r_e}$ (Hence g_m increases as I_E increases).

(c) $r_{b'e} = \frac{r_e}{1 - \alpha_{dc}}$ (Hence $r_{b'e}$ decreases as I_E increases).

(d) $C_{b'e} r_{b'e}$ = Constant (Hence $C_{b'e}$ increases as I_E increases).

In the Π-model, forward transfer is indicated by the current generator $g_m v_{b'e}$. The transconductance g_m, which at high frequencies actually becomes y_m, is considered independent of frequency and equal to the intrinsic low frequency transconductance $g_m = \frac{\alpha}{r_e}$ of the transistor. The generator $g_m v_{b'e}$ is not constant with increasing frequency because of the low-pass filter effect of $r_{bb'}$ and $C_{b'e}$ at the input circuit. If a comparison is made between the h-parameters type circuit model and the hybrid-Π, it can be concluded that $g_m v_{b'e}$ is not frequency dependent. But this analogy[16] breaks down as the frequency increases and g_m becomes complex, and takes the form of:

$$g_m = \frac{q\, I_C/kT}{1 - j\, \omega/2.4\, \omega_\alpha} \qquad \ldots (7)$$

where ω_α is the upper radian frequency. The transconductance g_m is no longer in the form shown for higher frequencies than alpha cut-off frequency f_α; but it is considered in the very complex form of y_m[16].

CHAPTER II

EQUIVALENT NOISE RESISTANCE OF A TRANSISTOR IN A COMMON-EMITTER CONFIGURATION

The noise current generators i_1 and i_2 are superimposed on a T-model representation of the common-emitter configuration:

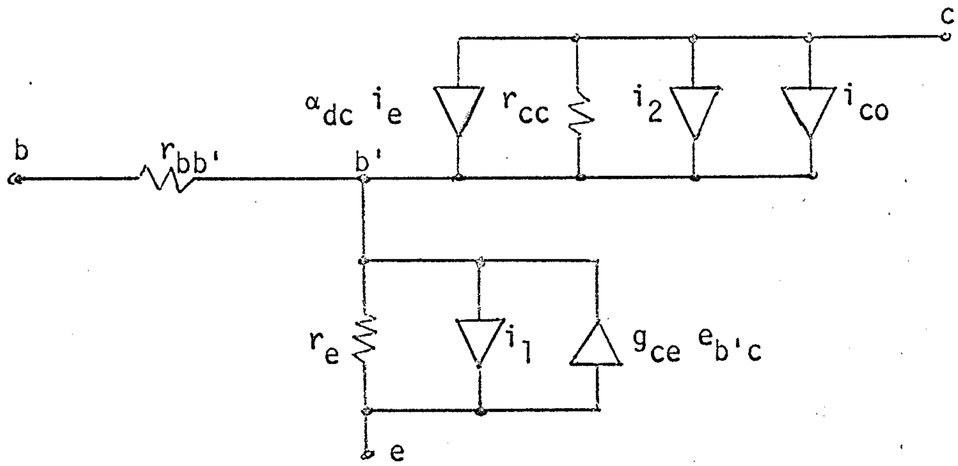

Figure 5

REPRESENTATION OF A T-MODEL WITH NOISE CURRENT GENERATORS SUPERIMPOSED

These noise current generators i_1 and i_2 are superimposed on the hybrid-π model of Figure 4. Now splitting the i_2 current generator into two parts, the model becomes

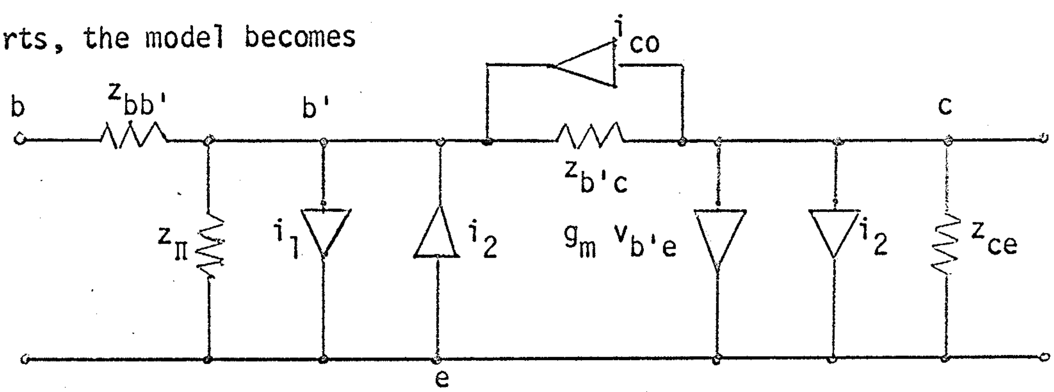

Figure 6

REPRESENTATION OF A HYBRID-π MODEL WITH NOISE CURRENT GENERATORS SUPERIMPOSED

The mean square values of the noise current i_1 and i_2 in the T-model are defined by VAN DER ZIEL[5] thus:

$$\overline{i_1^2} = 4kT(g_e - g_{eo})\Delta f + 2q(I_E + 2I_{EE})\Delta f \qquad \ldots (4)$$

$$\overline{i_2^2} = 2q\, I_C\, \Delta f \qquad \ldots (6)$$

$$\overline{i_1^* i_2} = 2kT\alpha y_e \Delta f \qquad \ldots (8)$$

where α is the a.c. intrinsic current gain and y_e is the emitter admittance.

When $$g_{eo} = \frac{q(I_E + I_{EE})}{kT}$$

is substituted into equation (4), it yields

$$\overline{i_1^2} = (4kT\, g_e - 2q\, I_E)\Delta f. \qquad \ldots (9)$$

Now, for the hybrid-Π model of Figure 6, the noise current generators become:

$$\overline{i_b^2} = \overline{(i_1 - i_2)(i_1 - i_2)^*} \qquad \ldots (10)$$

$$\overline{i_a^2} = 2q\, I_{CC}\, \Delta f \qquad \ldots (11)$$

$$\overline{i_c^2} = 2q\, I_C\, \Delta f. \qquad \ldots (12)$$

The noise currents $\overline{i_a^2}$, $\overline{i_b^2}$ and $\overline{i_c^2}$ are due to the d.c. current fluctuations.

A convenient way of rating the relative noisiness of circuits is by relating signal to noise power ratios of input and output. Therefore, a noise figure can be defined:

$$F = \frac{\dfrac{\text{source-available signal power}}{\text{source-available noise power}}}{\dfrac{\text{output-available signal power}}{\text{output-available noise power}}} \qquad \ldots (13)$$

The noise figure F may be evaluated several ways. One way to calculate F is by transferring all the noise sources to the input. The equivalent input noise generator will produce exactly the same noise at the output.

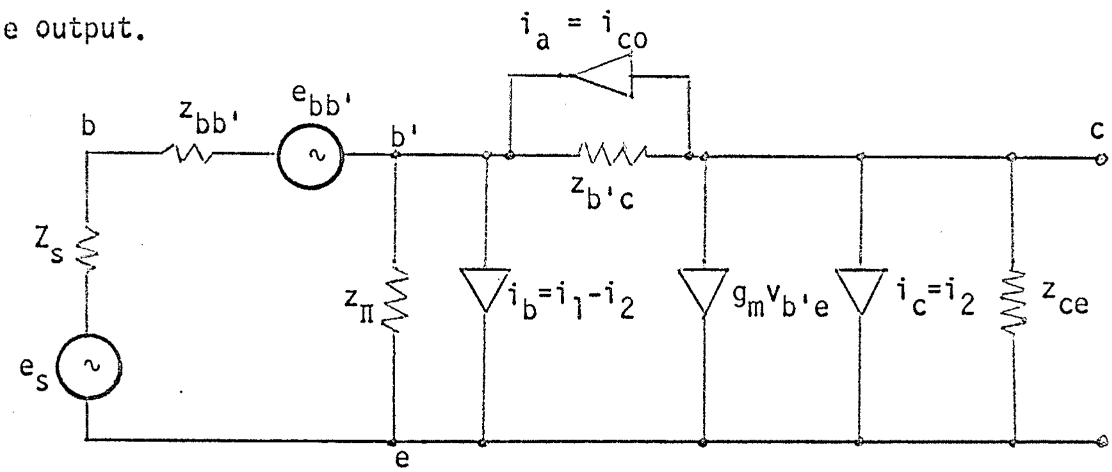

Figure 7

REPRESENTATION OF A HYBRID-Π MODEL WITH NOISE GENERATORS SUPERIMPOSED

The thermal noise generators due to the real part of the source impedance Z_s and the base impedance $z_{bb'}$ are

$$\overline{e_s^{\ 2}} = 4kT \text{ Re } \{Z_s\} \ \Delta f \qquad \text{... (14)}$$

$$\overline{e_{bb'}^{\ 2}} = 4kT \text{ Re } \{z_{bb'}\} \ \Delta f. \qquad \text{... (15)}$$

Since $\overline{e_s^{\ 2}}$ and $\overline{e_{bb'}^{\ 2}}$ are already at the input, only $\overline{i_b^{\ 2}}$, $\overline{i_c^{\ 2}}$ and $\overline{i_a^{\ 2}}$ need to be transferred to the input.

The feedback term $z_{b'c}$ can be neglected because it does not affect the noise figure.

i_b is replaced by an equivalent generator e_y at the input, where

$$e_y = i_b \ (Z_s + z_{bb'}). \qquad \text{... (16)}$$

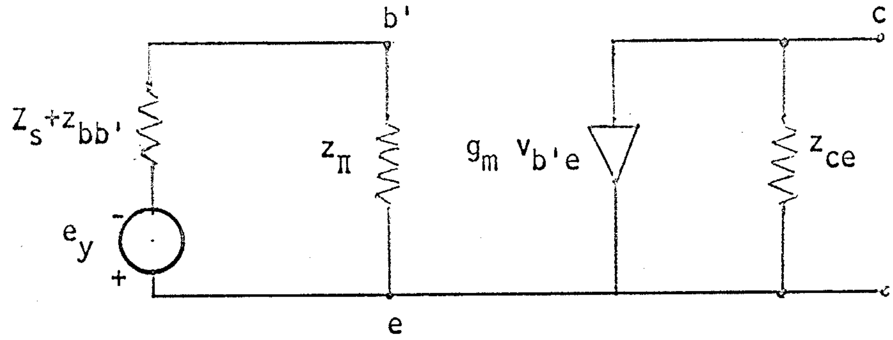

Figure 8

TRANSFORMATION OF NOISE-CURRENT GENERATOR i_b TO THE INPUT

i_c is replaced by an equivalent generator e_z at the input:

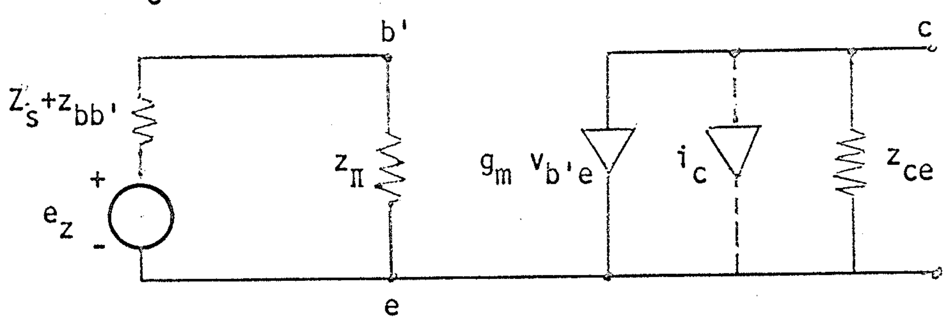

Figure 9

TRANSFORMATION OF NOISE-CURRENT GENERATOR i_c TO THE INPUT

Since
$$v_{b'e} = \frac{e_z}{Z_s + z_{bb'} + z_\Pi} \cdot z_\Pi$$

and
$$i_2 = g_m v_{b'e}$$

then
$$e_z = i_c \left(\frac{Z_s + z_{bb'} + z_\Pi}{g_m z_\Pi}\right) \qquad \ldots (17)$$

For the noise current generator i_a in the model, an equivalent generator e_w is placed at the input:

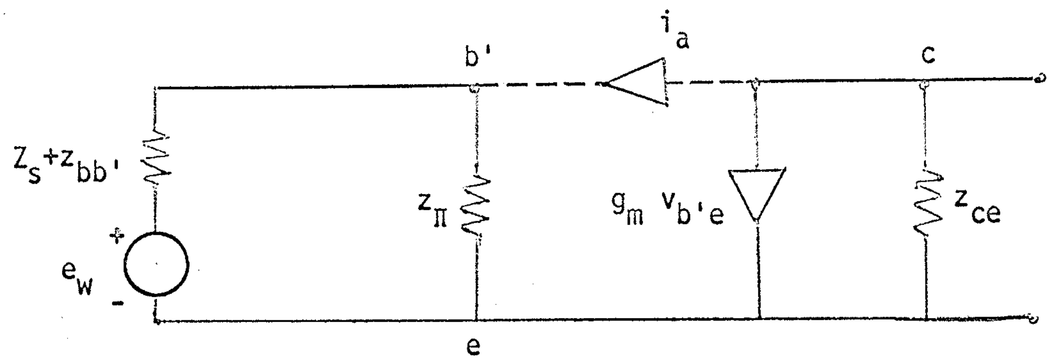

Figure 10

TRANSFORMATION OF NOISE-CURRENT GENERATOR i_a TO THE INPUT

Since

$$\frac{v_{b'e}}{Z_s + z_{bb'}} + \frac{v_{b'e}}{z_\Pi} = i_a = -(g_m\ v_{b'e} + \frac{v_c}{z_{ce}})$$

then

$$v_{b'e} = i_a \left[\frac{1}{\frac{1}{z_\Pi} + \frac{1}{Z_s + z_{bb'}}}\right] .$$

Now, if i_a is considered open circuit in Figure 10, then

$$v_{b'e} = \frac{e_w}{Z_s + z_{bb'} + z_\Pi}\ z_\Pi .$$

Noting that

$$-\frac{v_c}{z_{ce}} = g_m\ v_{b'e}$$

it follows that

$$e_w = i_a \left[\frac{(Z_s + z_{bb'})(1 + g_m\ z_\Pi) + z_\Pi}{g_m\ z_\Pi}\right] . \qquad \ldots (18)$$

All the equivalent noise generators now appear at the input.

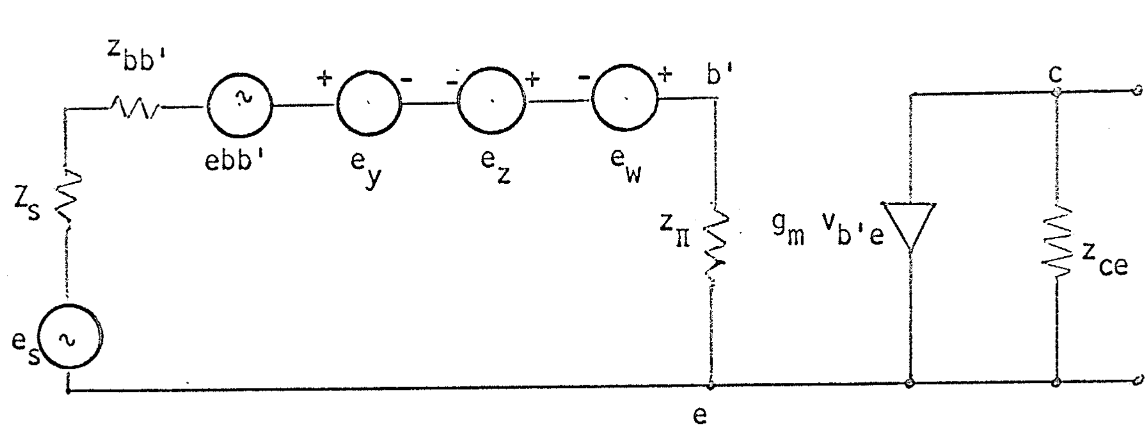

Figure 11

FICTITIOUS NOISE GENERATORS OF A TRANSISTOR

From Figure 11,

$$e_n = e_s + e_b - e_y + e_z + e_w \qquad \ldots (19)$$

Now, if $\overline{e_n^2} = 4kT\, R_n\ \Delta f$, where R_n is the equivalent noise resistance; the noise figure F may be found by the ratio of $\overline{e_n^2}$ to $\overline{e_s^2}$.

$$F = \frac{\overline{e_n^2}}{\overline{e_s^2}} = \frac{R_n}{R_s} \qquad \ldots (20)$$

A significant cross-correlation $\overline{i_b{}^*i_c}$ results at high frequencies. (Ref. #17).

where $\overline{i_b{}^*i_c} = \overline{(i_1 - i_2)^*i_2}$

or $\overline{i_b{}^*i_c} = 2kT\alpha y_e\ \Delta f - 2q\ I_C\ \Delta f$.

If $g_{mo} = \dfrac{qI_C}{kT}$ and $g_m = \alpha y_e$

then $\overline{i_b{}^*i_c} = 2kT\ (g_m - g_{mo})\ \Delta f$. $\qquad \ldots (21)$

Only the fictitious noise generators e_y and e_z are correlated. The multiplication of these generators results the cross-correlation $\overline{i_b{}^*i_c}$ term. From the quadratic addition of independent generators results

$$\overline{e_n^2} = \overline{e_s^2} + \overline{e_{bb'}^2} + \overline{e_y^2} + \overline{e_z^2} - \overline{e_y{}^*e_z} - \overline{e_y e_z{}^*} + \overline{e_w^2}. \qquad \ldots (22)$$

For silicon transistors, I_{CC} is very low and therefore the contribution of $\overline{e_w^2}$ to the equivalent noise generator may be neglected:

$$\overline{e_n^2} = \overline{e_s^2} + \overline{e_{bb'}^2} + \overline{i_b^2}\left|Z_s + z_{bb'}\right|^2 +$$

$$\overline{i_c^2}\left|\frac{Z_s + z_{bb'} + z_\Pi}{g_m z_\Pi}\right|^2 - 2\,\mathrm{Re}\,\{\overline{e_y{}^*e_z}\} \qquad \ldots (23)$$

If the $\overline{i_b^2}\left|Z_s + z_{bb'}\right|^2$ term is considered,

then $\left|Z_s + z_{bb'}\right|^2\{\overline{(i_1 - i_2)(i_1 - i_2)^*}\}$

$$= \left|Z_s + z_{bb'}\right|^2\{2q|-I_B|\Delta f + 2kT(2g_e - \alpha^* y_e{}^* - \alpha y_e)\}$$

where the term $(2g_e - \alpha^* y_e{}^* - \alpha y_e)$ is negligible.

Considering the $-2\,\mathrm{Re}\,\{\overline{e_y{}^*e_z}\}$ term:

$$-\,2\,\mathrm{Re}\,\{\overline{i_b{}^*i_c}\,(Z_s + z_{bb'})^*\,(\frac{Z_s + z_{bb'} + z_\Pi}{g_m z_\Pi})\}$$

$$= -\,4kT\Delta f\,\mathrm{Re}\,\{(g_m - g_{mo})(Z_s + z_{bb'})^*(\frac{Z_s + z_{bb'} + z_\Pi}{g_m z_\Pi})\}\,.$$

Using $F = \dfrac{\overline{e_n^2}}{\overline{e_s^2}} = \dfrac{R_n}{R_s}$,

it follows that

$$F = 1 + \frac{r_{bb'}}{R_s} + \frac{q\,I_B}{2kT\,R_s}\left|Z_s + z_{bb'}\right|^2$$

$$+ \frac{q\,I_C}{2kT\,R_s}\left|\frac{Z_s + z_{bb'} + z_\Pi}{g_m z_\Pi}\right|^2$$

$$- \frac{\mathrm{Re}}{R_s}\{(g_m - g_{mo})(Z_s + z_{bb'})^*(\frac{Z_s + z_{bb'} + z_\Pi}{g_m z_\Pi})\} \qquad \ldots (24)$$

The noise-figure equation is a function of R_s and X_s. Minimized values of F may be found by differentiating the noise-figure equation to obtain $\frac{\partial F}{\partial R_s}$ and $\frac{\partial F}{\partial X_s}$. After a few simplifications, it can be shown that:

$$R_{s_{opt}}^{\;2} \cong (r_{bb'} + r_{\Pi})^2 + (X_s + x_{\Pi})^2$$

$$+ 2g_m[r_{bb'}(r_{\Pi}^{\;2} + x_{\Pi}^{\;2}) + r_{\Pi}(r_{bb'}^{\;2} + X_s^{\;2})] \qquad \ldots (25)$$

and

$$X_{s_{opt}} \cong \frac{-x_{\Pi}}{1 + 2\, g_m\, r_{\Pi}} \; . \qquad \ldots (26)$$

If the reactance $x_{\Pi} >> r_{\Pi}$, and the optimum source reactance is used,

$$X_{s_{opt}} = \frac{-x_{\Pi}}{1 + 2\, g_m\, r_{\Pi}}$$

and

$$R_{s_{opt}} = - x_{\Pi} \sqrt{2\, g_m(r_{bb'} + \frac{r_{\Pi}}{1 + 2\, g_m\, r_{\Pi}})} \; . \qquad \ldots (27)$$

CHAPTER III

EXPERIMENTAL PROCEDURE

NOISE JIG

To perform the noise measurements, the following noise jig was designed:

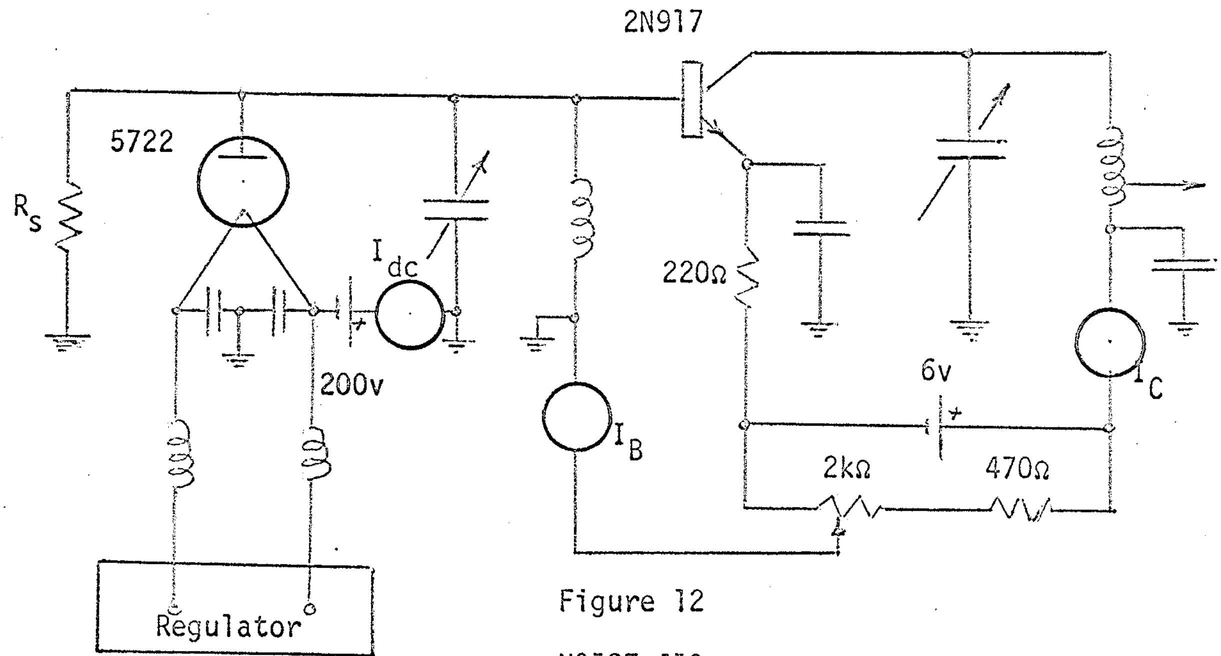

Figure 12

NOISE JIG

At 100 MHz, the inductance of the leads is very critical and therefore careful lay-out must be considered. The source impedance Z_s was simulated by a parallel-tuned LC circuit damped with metal-film resistances. Metal-film resistances were not available beyond 500 ohms; therefore a carbon-film rod resistance was used. At low frequencies, the base of the transistor is shorted to ground by the coil of the tank circuit. The coil suppresses low frequency flicker-noise components which could interact with high frequency noise (cross-modulation). The 5722 noise diode was placed at the input of the transistor. The d.c. path for the noise diode is provided through the RF choke. To minimize variations in plate current, the filament of the noise diode, which has a non-linear resistance with respect to the temperature, was fed from a constant current source:

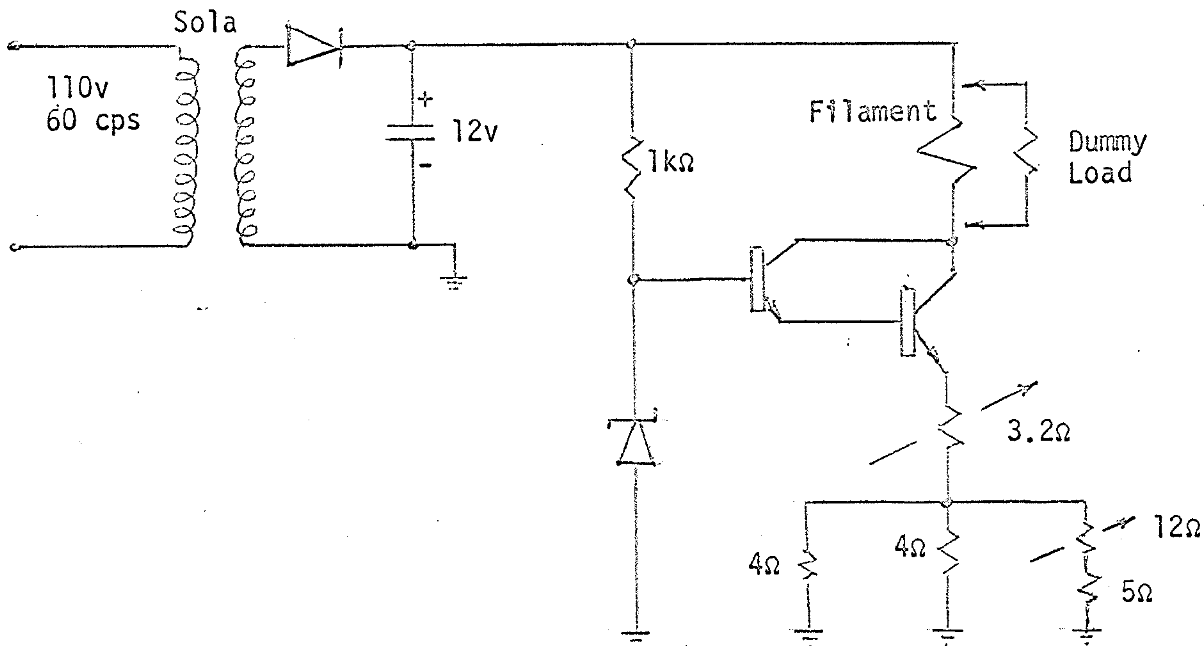

Figure 13

REGULATOR

A Sola transformer was used to compensate for line voltage variations. Corrective feedback was obtained by the emitter bias resistance R_E and large gain was obtained by the Darlington connection of the transistors.

NOISE MEASUREMENT METHOD

The source impedance was measured using a Wayne-Kerr Model B-801 bridge. The noise jig was connected to a converter, followed by a preamplifier and a 30 MHz. receiver with a precision attenutator.

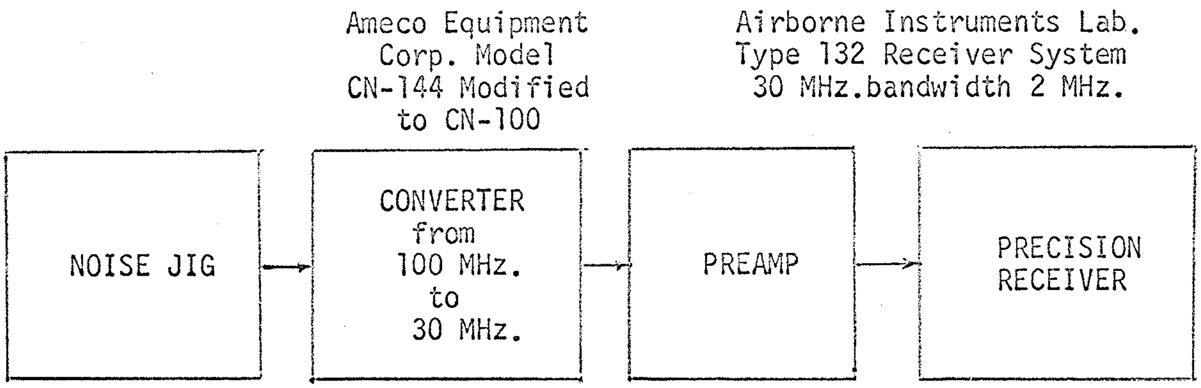

Figure 14

BLOCK DIAGRAM OF THE NOISE-MEASURING APPARATUS

Drift in the converter gain contributed some error to the measurements, but was minimized by the use of a large Sola transformer.

Noise measurements were made by doubling the output noise power. Now if P_o represents the output noise power, when the noise diode filament current is turned off, and the d.c. diode current I_{dc} is equal to zero,

then $$P_o = (4kT\ R_s \Delta f)(AF) \qquad \ldots (28)$$

where A is the power gain of the system and F is the noise figure of the system.

If P_d is the output noise power for a given d.c. diode current I_{dc} , then by superposition

$$P_d = (4kT\ R_s \Delta f)(AF) + 2q\ I_{dc} \Delta f\ |Z_s|^2\ A \qquad \ldots (29)$$

If the output noise power is doubled

ie. $$P_d = 2\ P_o ,$$

and $$\frac{P_d}{P_o} = 1 + \frac{q\ I_{dc}|Z_s|^2}{2kT\ F\ R_s}$$

from which $$F = \frac{q}{2kT} I_{dc} \frac{|Z_s|^2}{R_s} \quad . \qquad \text{... (30)}$$

It can also be seen that

$$\overline{e_n^{\ 2}} = 4kT\ R_n \Delta f = 2q\ I_{dc} \Delta f\ |Z_s|^2$$

$$F = \frac{R_n}{R_s} = \frac{q}{2kT} I_{dc} \frac{|Z_s|^2}{R_s}$$

For the case of the source impedance Z_s equal to the source resistance R_s

$$F = 19.35\ I_{dc}\ R_s \qquad \text{... (31)}$$

at $T = 293^{\circ}K$ (room temperature).

CORRECTION FOR BACKGROUND NOISE

The output noise power contains a background noise power, therefore a compensation for the background noise must be considered when the output noise power is doubled.

If M is the output noise-power reading and M_b is the background noise-power reading, then

$$\frac{M_b}{M_1} = \frac{1}{k}$$

where k is the ratio of the first output noise-power reading to the background noise-power reading. If the first output noise-power reading M_1 is doubled then the ratio of the second output noise-power reading M_2 to M_1 becomes

$$\frac{M_2}{M_1} = \frac{2\ M_1 - M_b}{M_1}$$

or $$\frac{M_2}{M_1} = 2 - \frac{1}{k} \quad . \qquad \text{... (32)}$$

CALCULATION OF INTRINSIC g_m FROM EXTRINSIC y_m MEASUREMENTS

Upon examination of the hybrid-Π model, it can be seen that the extrinsic transadmittance y_m as obtained from measurements is not the intrinsic g_m as defined in the model. This is due to the base impedance $z_{bb'}$ which forms the low-pass filter with z_Π in parallel with the feedback impedance $z_{b'c}$. Therefore, the following calculation has to be made:

The output is short-circuited in the y_m measurements.

Now
$$y_m = \frac{i_c}{v_{in}} .$$

But from the Π-model, it can be shown that

$$v_{b'e} = \frac{v_{in}}{z_{bb'} + z_\Pi // z_{b'c}} \; z_\Pi // z_{b'c} .$$

Now, since $\quad g_m v_{b'e} = i_c$

then
$$g_m = y_m \left(1 + \frac{z_{bb'}}{z_\Pi // z_{b'c}}\right) . \qquad \ldots (33)$$

g_m of equation (33) was still complex; therefore, the magnitude of g_m is considered. Since the input impedance $z_{in} = z_{bb'} + z_\Pi // z_{bb'}$ when the output is short-circuited, then

$$g_m = \left| y_m \left(\frac{z_{in}}{z_{in} - z_{bb'}}\right) \right| . \qquad \ldots (34)$$

CHAPTER IV

EXPERIMENTAL RESULTS

The input impedance z_{in} and the transadmittance y_m of the transistor (2N917) were measured, using the high-frequency G.R. Transfer-Function and Immittance Bridge Type 1607-A. The measurements were done with three different collector currents 100μA, 300μA and 1 mA.

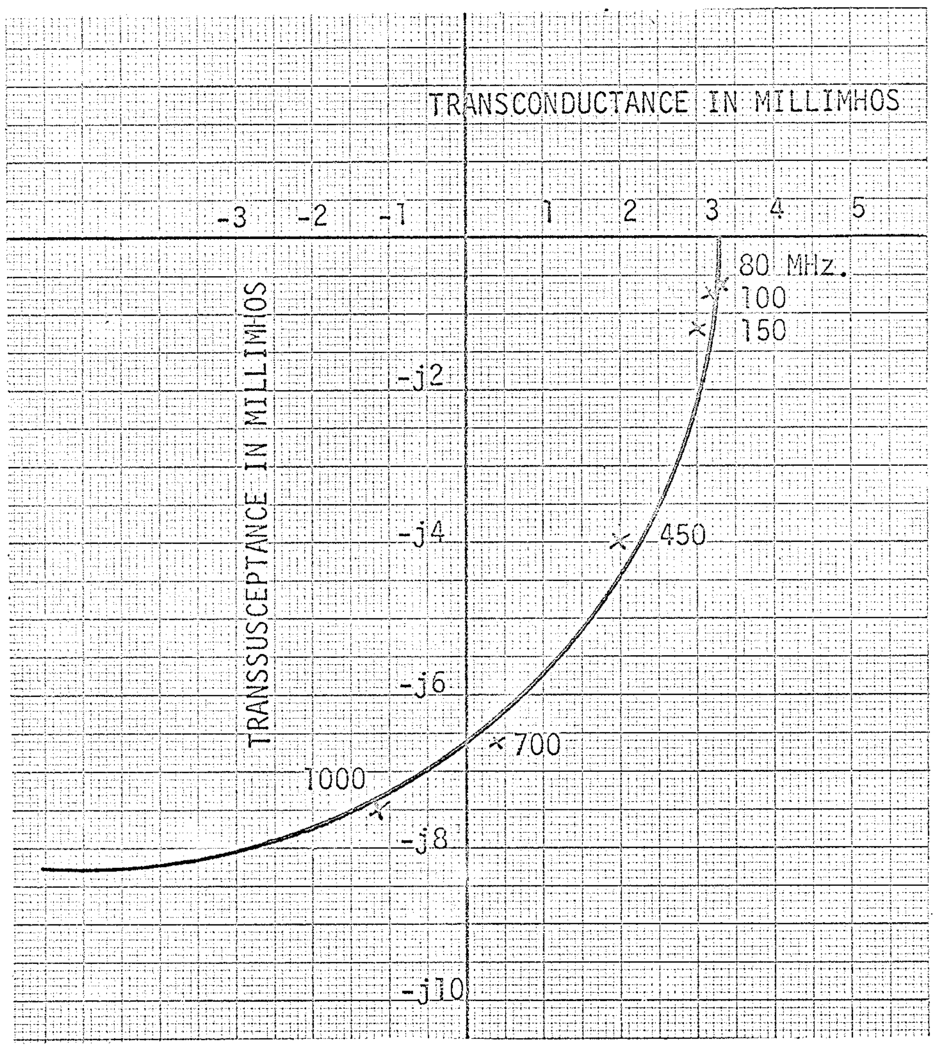

Figure 15

MEASURED TRANSADMITTANCE (y_m) for I_C = 100μA

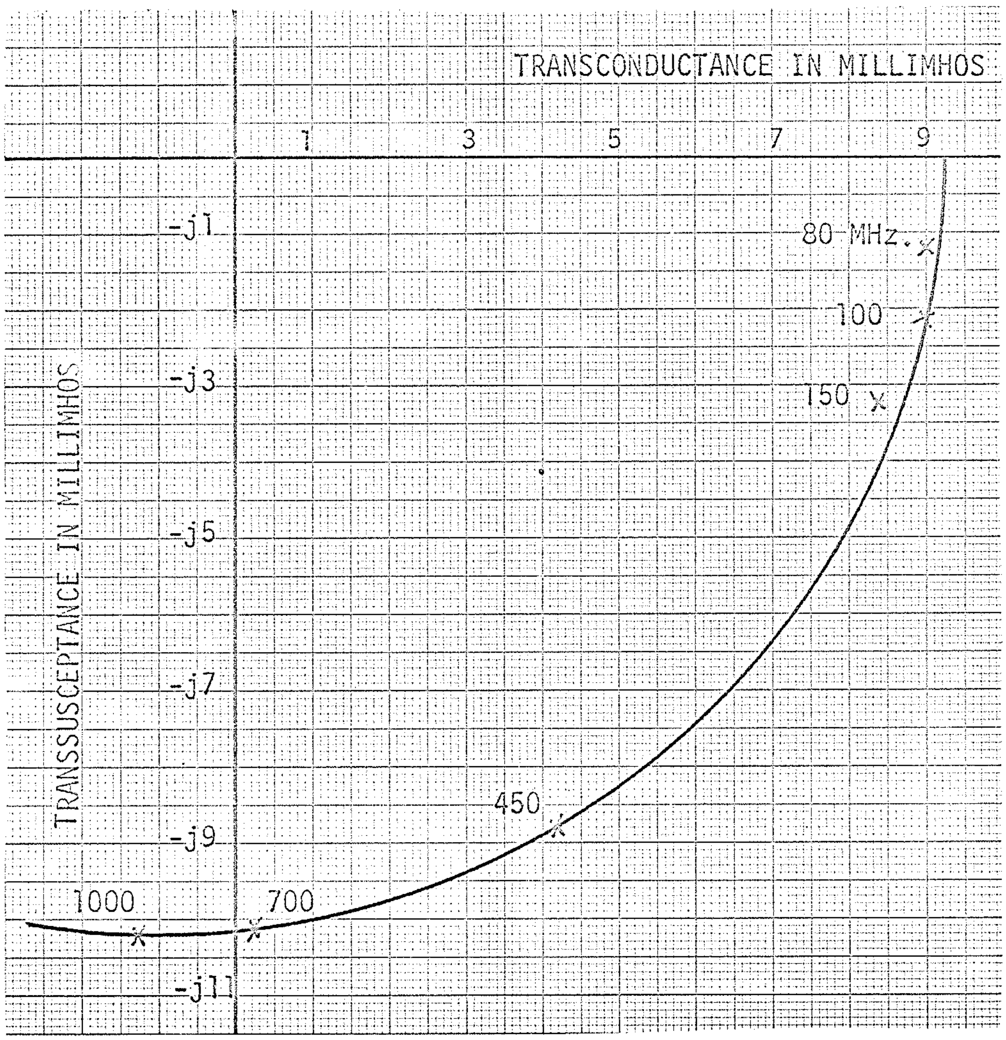

Figure 16

MEASURED TRANSADMITTANCE (y_m) for I_C = 300μA

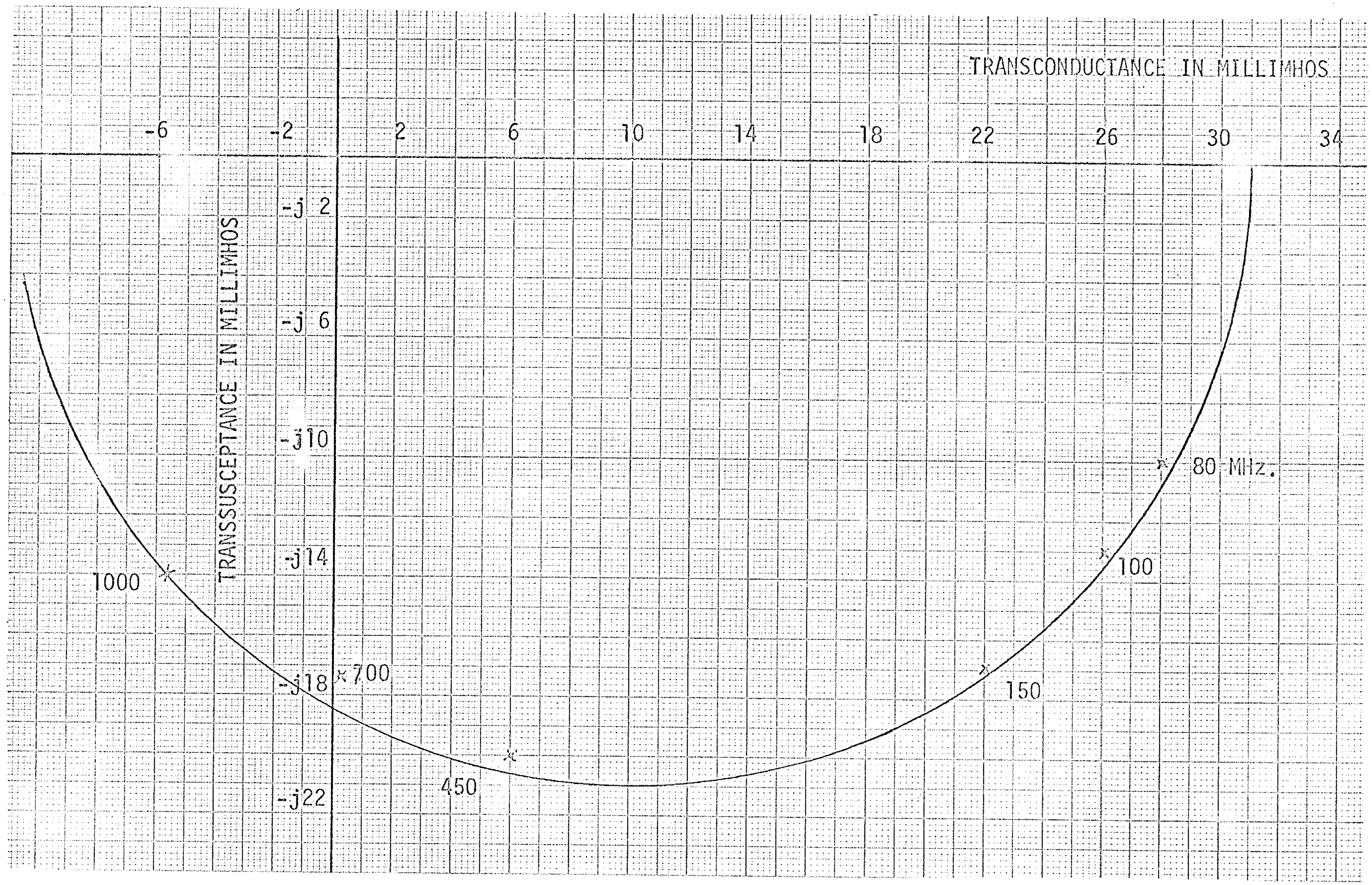

Figure 17

MEASURED TRANSADMITTANCE (y_m) for I_C = 1 mA

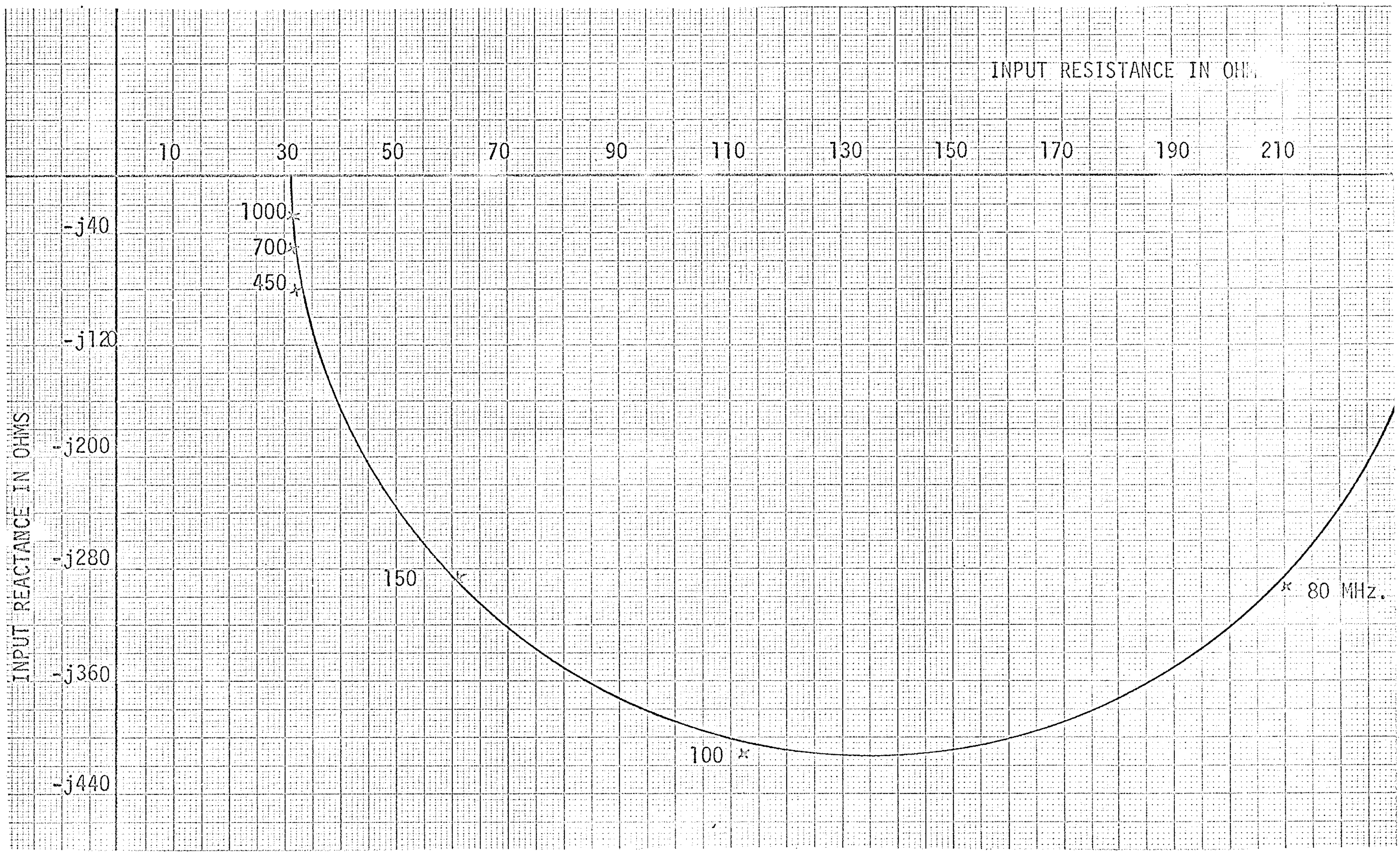

Figure 18

MEASURED INPUT IMPEDANCE FOR I_C = 100μA

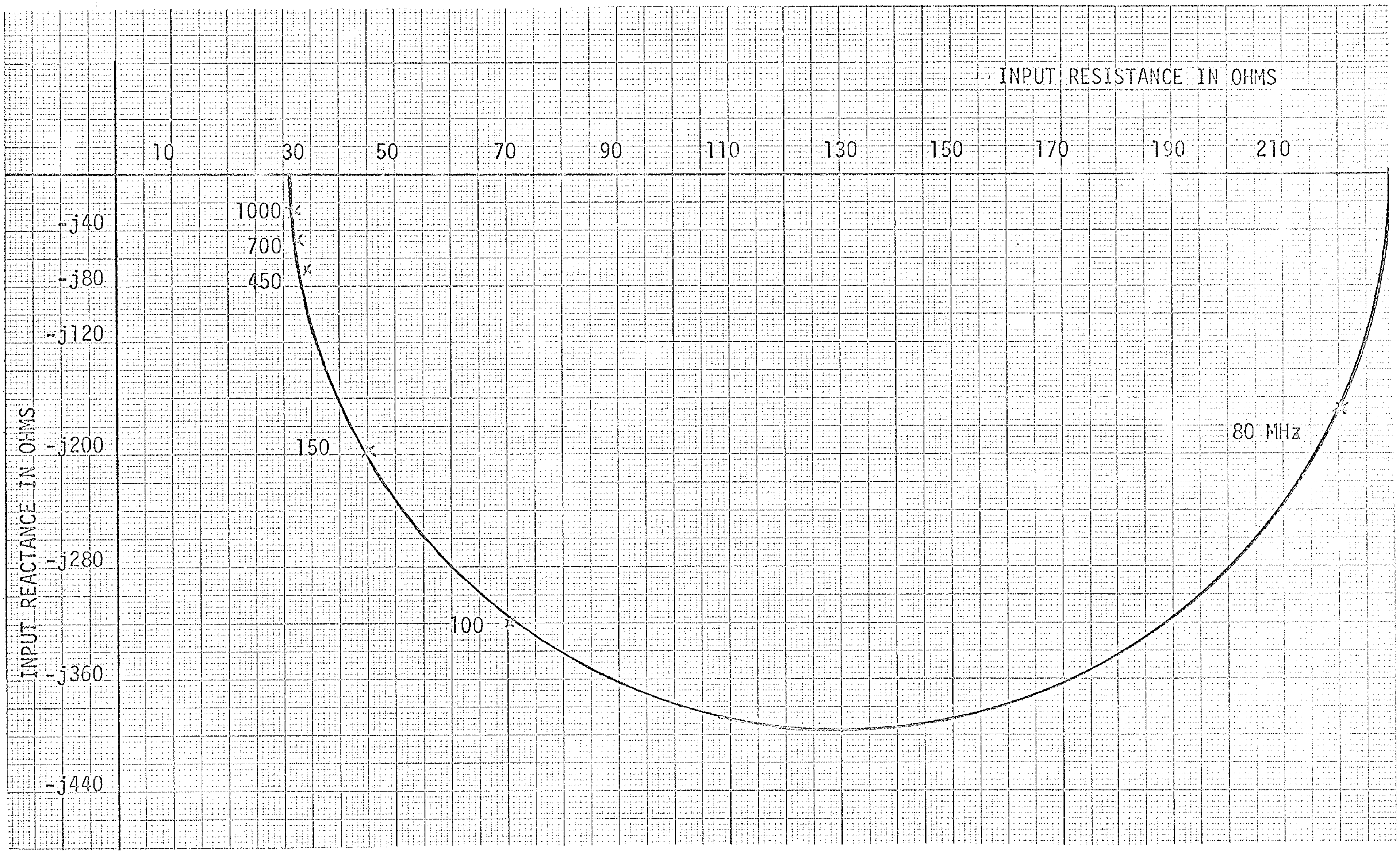

Figure 19

MEASURED INPUT IMPEDANCE for I_C = 300μA

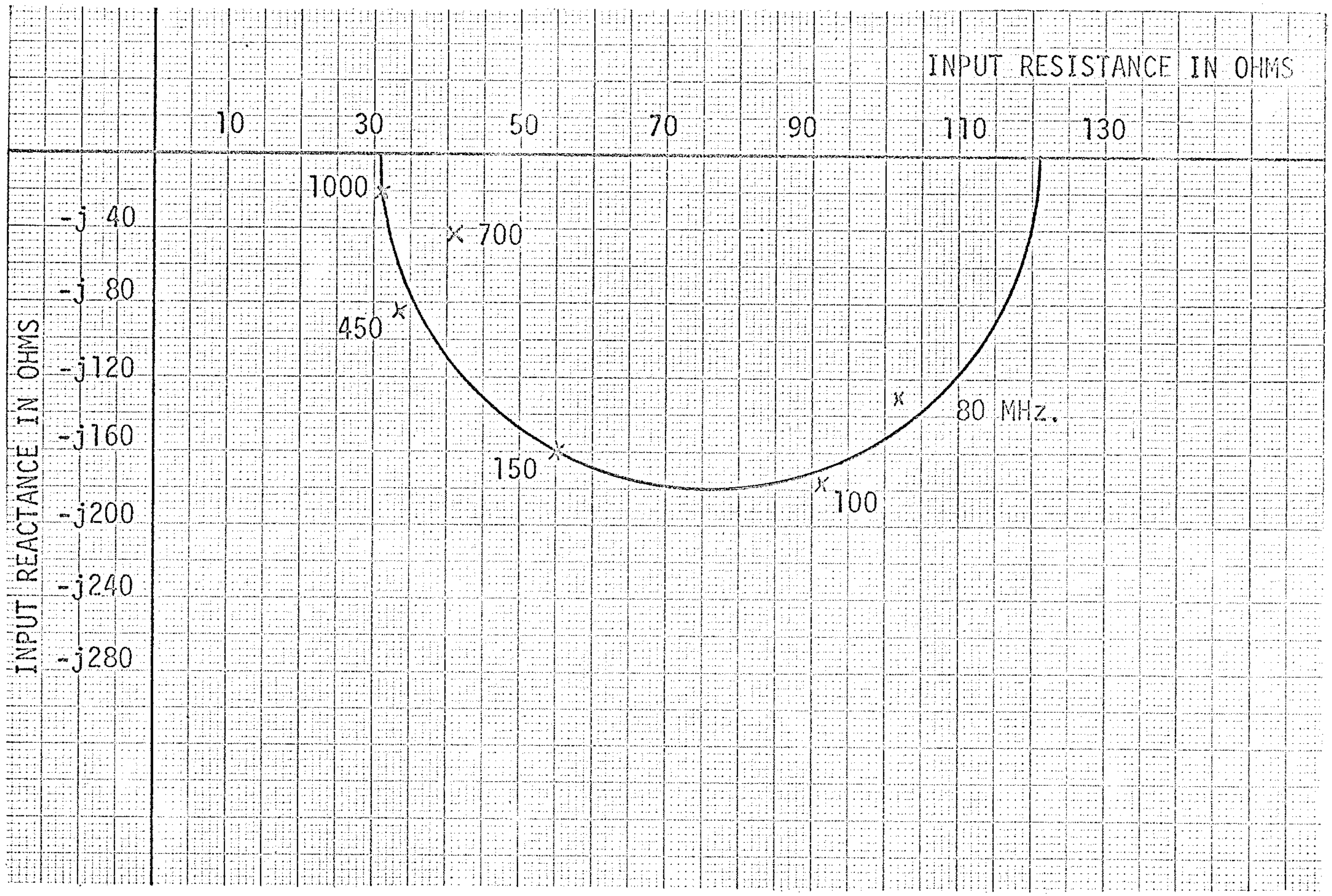

Figure 20

MEASURED INPUT IMPEDANCE for $I_C = 1$ mA

It can be shown that for a constant noise figure F, equation (24) yields a circle in $X_s - R_s$ plane. Circled regions converge upon a point, where F is a minimum. Measured and calculated noise-figure values are within 0.5 db of difference.

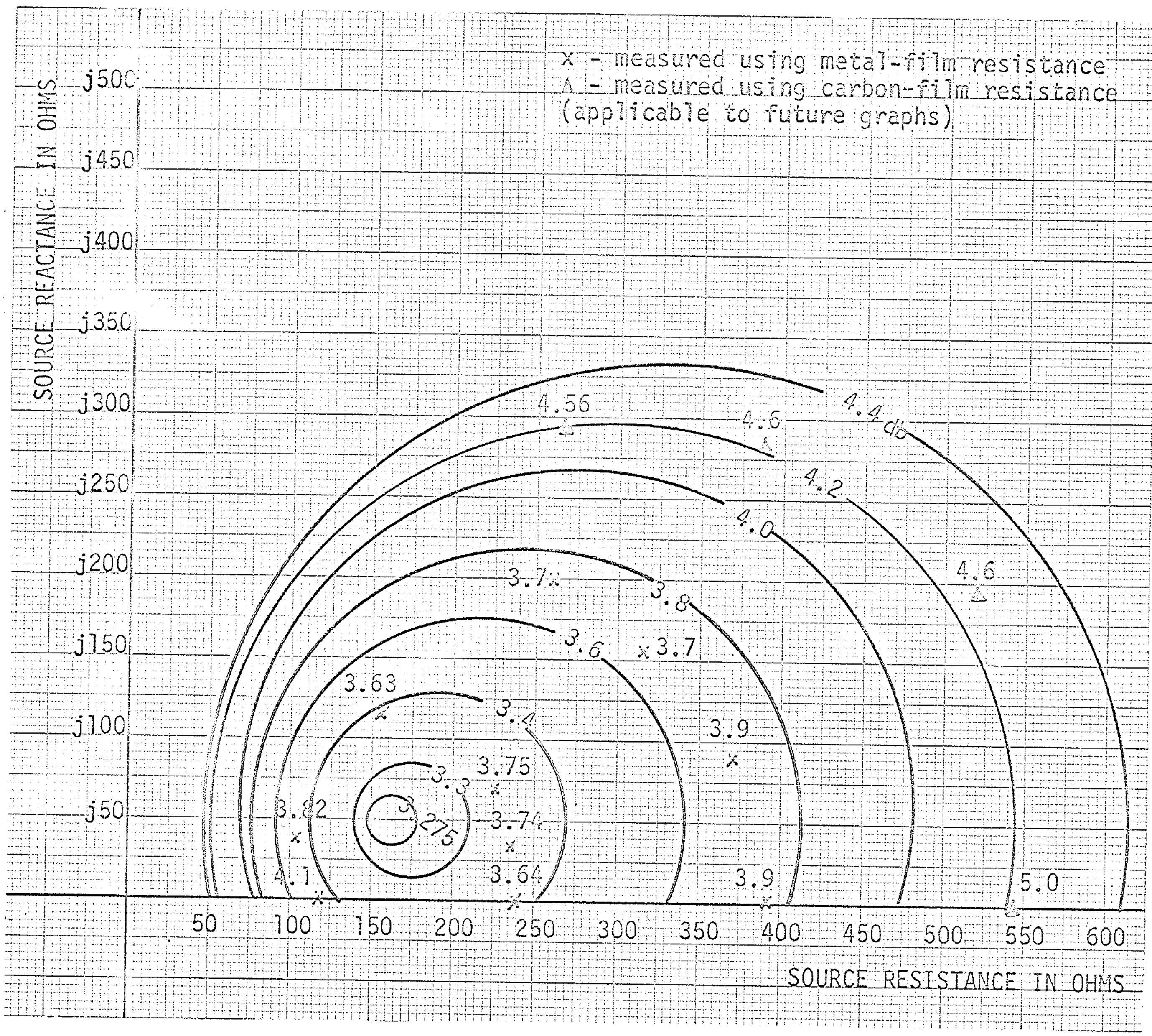

Figure 21

CONTOURS OF CONSTANT NOISE FIGURE FOR 2N917 TRANSISTOR (I_C = 1mA)

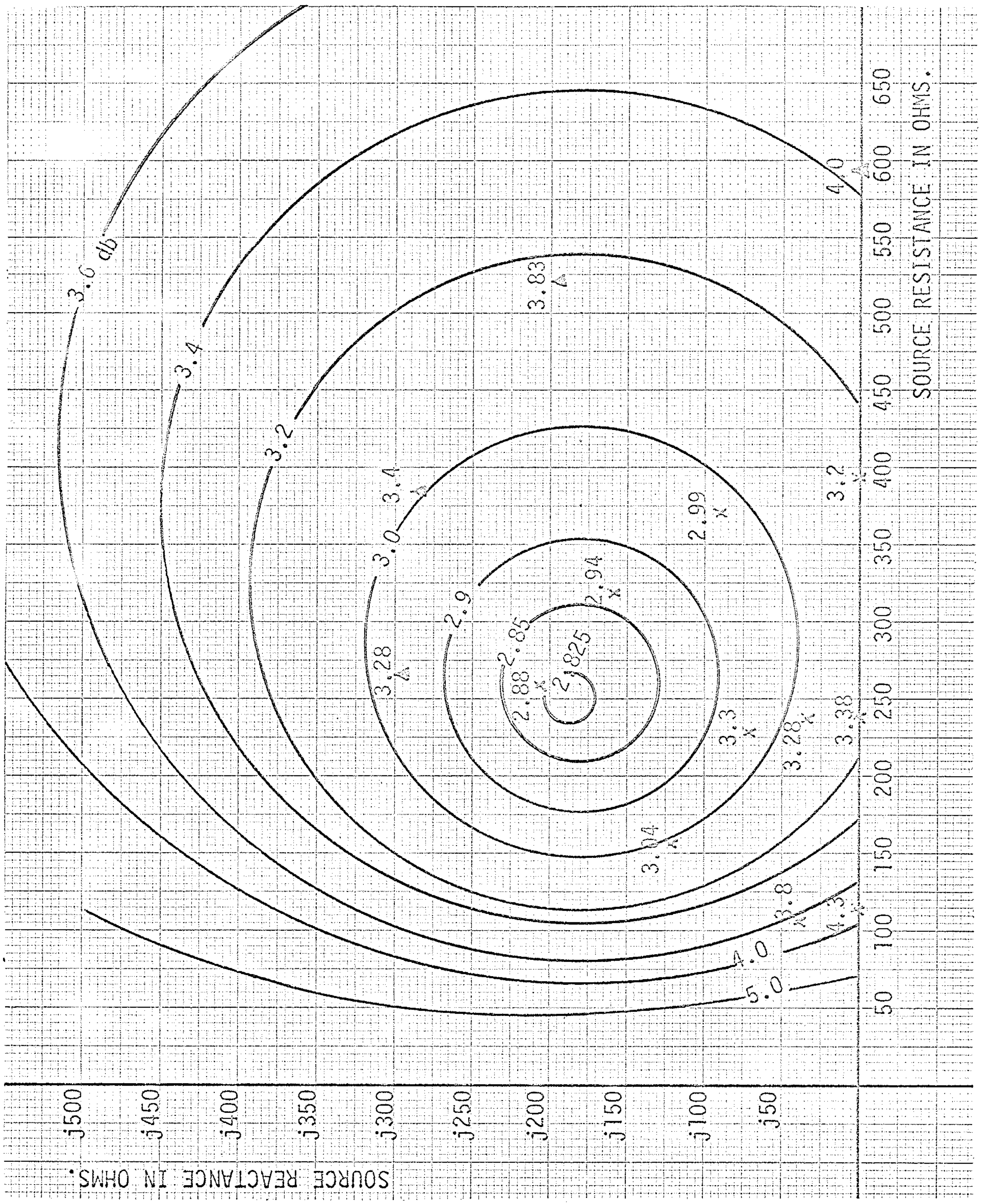

Figure 22

CONTOURS OF CONSTANT NOISE FIGURE FOR I_C = 300μA

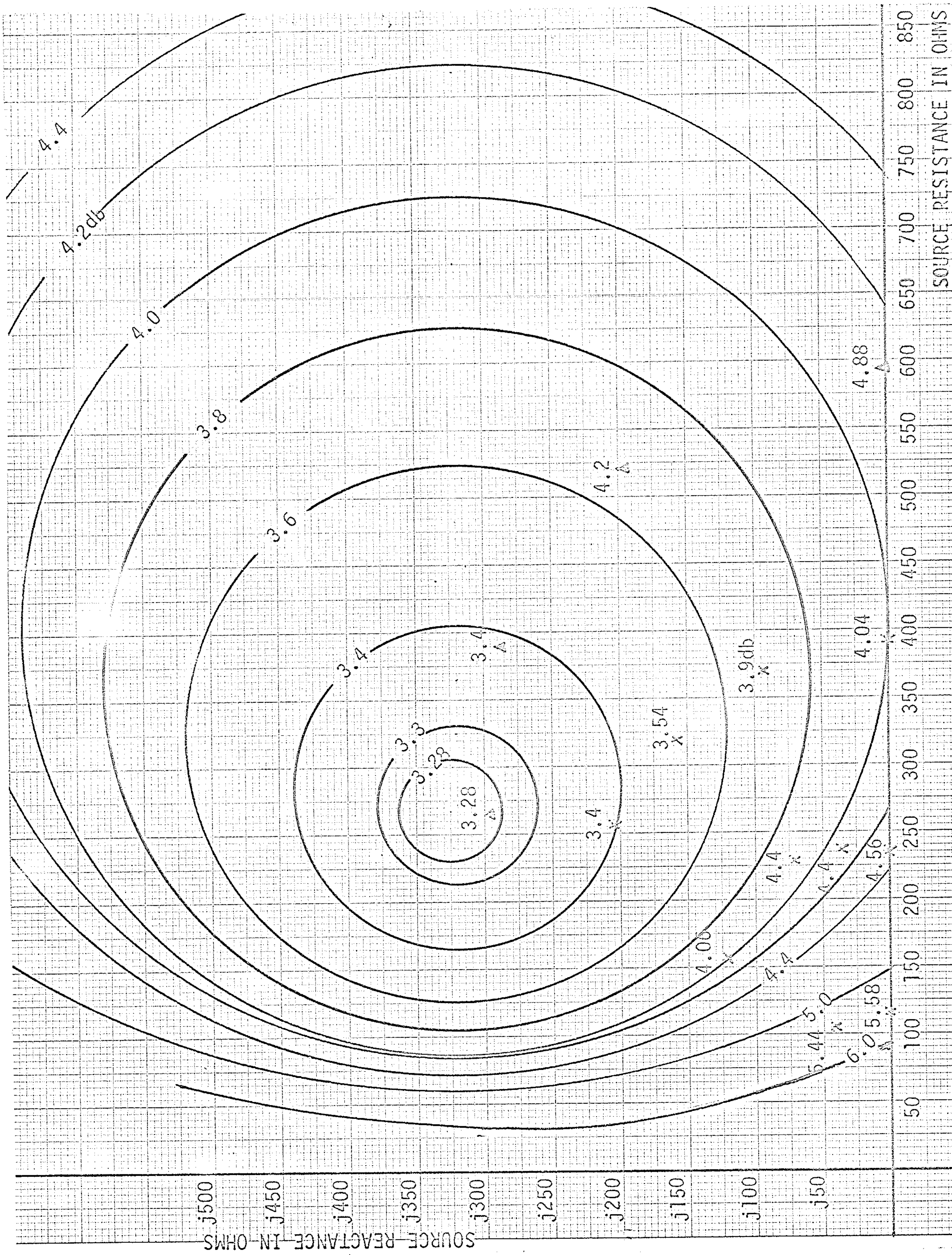

Figure 23

CONTOURS OF CONSTANT NOISE FIGURE FOR $I_C = 100\mu A$

CHAPTER V

CONCLUSION

The high-frequency noise behaviour of the UHF silicon drift transistor 2N917 used in the investigation obeys the theory within reasonable experimental error. Since the calculated and the measured noise figure values of this transistor are within 0.5 db., it can be concluded that the effects of $x_{bb'}$, I_{CC}, and recombination current I_R are negligible for this transistor. At this frequency, the contribution of the cross-correlation to the noise figure is quite significant, especially at high collector currents.

It was expected that the intrinsic transconductance g_m calculated from extrinsic transadmittance y_m measurements would become complex at 100 MHz. Calculations based on extrinsic transadmittance measurements showed that g_m had phase angles between 3^o and 12^o which could be within experimental errors. However, at high R_s - values (2kΩ), a complex g_m in the noise figure expression produces a negative noise-figure value which is physically impossible. Thus, only the magnitude of g_m is considered for the calculations.

The input impedance of the transistor in the common-emitter configuration is capacitive. In order to have a power match for minimum noise figure, an inductive source impedance was introduced. It is interesting to note that introducing inductive source reactance at low currents reduces the noise figure as $R_{s_{opt}}$ is kept approximately the same.

In the hybrid-Π model, z_Π is a function of emitter current I_E ; thus, the noise figure is a function of I_E . A collector current value of approximately 450 μA gives the minimum noise figure for this transistor.

BIBLIOGRAPHY

1. Hanson, "Shot Noise in Transistors", Proc. IRE, Vol. 45- 1957, pp. 1538-1542.

2. Nielsen, E.G., "Behaviour of the Noise Figure in Junction Transistors", Proc. IRE., Vol.45, 1957, July, pp. 957-963, pp. 839-857 with correction 1509.

3. Van Der Ziel, "Noise in Junction Transistors", Proc. IRE., Vol. 46, 1958, March, pp. 1019-1038, pp. 589-594.

4. Van Der Ziel, Chennette, "Accurate Noise Measurements on Transistors", Proc. IRE., ED-9, 1962, pp. 123-128.

5. Van Der Ziel, "Shot Noise in Transistors", Proc. IRE., Vol. 48, Jan. 1960, pp. 114-115.

6. Schneider & Strutt, "Shot and Thermal Noise in Silicon and Germanium Transistors", Proc. IRE., Vol. 48, 1960, pp. 1731-1739.

7. Van Der Ziel, "Noise", Prentice Hall, 1954.

8. Gradner & Flyd, IEEE, Transactions, C-T, 1963, March, pp. 45-48.

9. Chennette, "Inductive Sources", Proc. IRE., Vol. 47, 1959, pp. 448-449.

10. Pritchard, Angell, Adler, Early and Webster, "Transistor Internal Parameters for Small Signal Representation", Proc.IRE, Vol. 49, No. 4, 1961, April, p. 725.

11. Joyce & Clarke, "Transistor Circuit Analysis", Addison-Wesley Pub. Co. Inc., copy Oct. 1961.

12. Schwartz, Mischa, "Information, Transmission, Modulation and Noise," McGraw-Hill Book Co., Inc. 1959.

13. Jakobschuk, A., Graduate Thesis, "HF Noise in Transistors", University of Minnesota, August 1964.

14. Swiontek, M.C. & Hassun, R., "The Influence of Transistor Parameters on Transistor Noise Performance", A Simplified Presentation. HP Journal.

15. Hyde, F., "The Physical Basis of Noise", "Noise in Electronic Devices", The Institute of Physics and Physical Society, by Chapman and Hall Ltd., London, Reinhold Publishing Corp., New York.

16. Nanavati, "An Introduction to Semiconductor Electronics", McGraw-Hill Book Co. Inc., 1963.

17. Thornton, DeWitt, Chenette, Lin, "CLT - Characteristics and Limitations of Transistors", SEEC Notes, John Wiley & Sons Inc., 1963.